


## Article

# CO<sub>2</sub> Injection for Enhanced Gas Recovery and Geo-Storage in Complex Tight Sandstone Gas Reservoirs

Linqiang Zhang <sup>1</sup>, Tongzhou Bai <sup>2</sup>, Qibin Zhao <sup>3</sup>, Xinghua Zhang <sup>4</sup>, Hanlie Cheng <sup>2,\*</sup>  and Zhao Li <sup>2</sup><sup>1</sup> China United Coalbed Methane Co., Ltd., Beijing 100011, China<sup>2</sup> COSL-EXPRO Testing Services Co., Ltd., Tianjin 300457, China<sup>3</sup> Exploration Department, CNOOC Co., Ltd., Beijing 100010, China<sup>4</sup> Tianjin Branch, CNOOC Co., Ltd., Tianjin 300459, China

\* Correspondence: chenghl@cosl-expro.com

**Abstract:** With the popularization of natural gas and the requirements for environmental protection, the development and utilization of natural gas is particularly important. The status of natural gas in China's oil and gas exploration and development is constantly improving, and the country is paying more and more attention to the exploitation and utilization of natural gas. The Upper Paleozoic tight sandstone in the Ordos Basin is characterized by low porosity, low permeability and a large area of concealed gas reservoirs. By injecting carbon dioxide into the formation, the recovery rate of natural gas can be improved, and carbon neutrality can be realized by carbon sequestration. Injecting greenhouse gases into gas reservoirs for storage and improving recovery has also become a hot research issue. In order to improve the recovery efficiency of tight sandstone gas reservoirs, this paper takes the complex tight sandstone of the Upper Paleozoic in the Ordos Basin as the research object; through indoor physical simulation experiments, carried out the influence of displacement rate, fracture dip angle, core permeability, core dryness and wetness on CO<sub>2</sub> gas displacement efficiency and storage efficiency; and analyzed the influence of different factors on gas displacement efficiency and storage efficiency to improve the recovery and storage efficiency. The research results show that under different conditions, when the injection pore volume is less than 1 PV, the relationship between the CH<sub>4</sub> recovery rate and the CO<sub>2</sub> injection pore volume is linear, and the tilt angle is 45°. When the injection pore volume exceeds 1 PV, the CH<sub>4</sub> recovery rate increases slightly with the increase in displacement speed, the recovery rate of CO<sub>2</sub> displacement CH<sub>4</sub> is between 87–97% and the CO<sub>2</sub> breakthrough time is 0.7 PV–0.9 PV. In low-permeability and low-speed displacement cores, the diffusion of carbon dioxide molecules is more significant. The lower the displacement speed is, the earlier the breakthrough time is, and the final recovery of CH<sub>4</sub> slightly decreases. Gravity has a great impact on carbon sequestration and enhanced recovery. The breakthrough of high injection and low recovery is earlier, and the recovery of CH<sub>4</sub> is about 3.3% lower than that of low injection and high recovery. The bound water causes the displacement phase CO<sub>2</sub> to be partially dissolved in the formation water, and the breakthrough lags about 0.1 PV. Ultimately, the CH<sub>4</sub> recovery factor and CO<sub>2</sub> storage rate are higher than those of dry-core displacement. The research results provide theoretical data support for CO<sub>2</sub> injection to improve recovery and storage efficiency in complex tight sandstone gas reservoirs.

**Keywords:** complex tight sandstone gas reservoirs; CO<sub>2</sub> geo-storage; enhanced natural gas recovery; physical simulation experiment



**Citation:** Zhang, L.; Bai, T.; Zhao, Q.; Zhang, X.; Cheng, H.; Li, Z. CO<sub>2</sub> Injection for Enhanced Gas Recovery and Geo-Storage in Complex Tight Sandstone Gas Reservoirs. *Processes* **2023**, *11*, 2059. <https://doi.org/10.3390/pr11072059>

Academic Editors: Tao Zhang, Zheng Sun, Dong Feng, Hung Vo Thanh and Wen Zhao

Received: 29 May 2023

Revised: 5 July 2023

Accepted: 7 July 2023

Published: 10 July 2023



**Copyright:** © 2023 by the authors. Licensee MDPI, Basel, Switzerland. This article is an open access article distributed under the terms and conditions of the Creative Commons Attribution (CC BY) license (<https://creativecommons.org/licenses/by/4.0/>).

## 1. Introduction

With the rapid development of the industrial society, the burning of a large amount of fossil fuels in human activities has led to the emission of a large amount of carbon dioxide into the atmosphere, resulting in global warming and a serious threat to people's living environment [1–4]. Natural gas is the cleanest fossil energy source, with high calorific value

and the same amount of electricity. The carbon dioxide emitted is only 50% of that of coal and 30% less than that of oil, which is conducive to achieving low-carbon goals. Natural gas also has advantages that renewable energy does not have: for example, wind energy and light energy are unstable, and their supply reliability is not as good as natural gas, which has strong compressibility and is convenient for transportation. The demand for natural gas is increasing year by year, and the gap between supply and demand of natural gas is prominent, so it is urgent to effectively develop and utilize natural gas. The importance of natural gas as a clean energy is increasing day by day [5]. At present, most natural gas mining uses depletion mining, and the recovery rate is low. Using carbon dioxide flooding can not only improve the recovery rate of natural gas but also realize effective carbon storage and reduce carbon emissions. By sequestering carbon dioxide, reducing CO<sub>2</sub> emissions in the atmosphere has become an important way to slow down global warming and climate change [6]. CO<sub>2</sub> geological storage is a technically feasible, efficient, safe and environmentally friendly emission reduction solution. Common sites for CO<sub>2</sub> geological storage include deep brine formations, depleted oil and gas reservoirs, unminable coal seams and deep-sea projects. If CO<sub>2</sub> is simply stored, the cost is high [7]. Therefore, the large-scale utilization of CO<sub>2</sub> greenhouse gas by improving oil and gas recovery while in storage has become a hot research topic. At present, the Ordos Basin, Tarim Basin and Luanghehai Basin in China have abundant natural gas reserves, and the storage potential of CO<sub>2</sub> is also huge [8]. Since the gas reservoir itself exists in the natural geological body that is most suitable for storing gaseous substances, the gas storage and sealing properties of the gas-bearing reservoir have also been fully confirmed in the natural gas occurrence and development stage [9]. The implementation of CO<sub>2</sub> storage has theoretical and practical advantages and practical feasibility. The existing results show that CO<sub>2</sub> is very unlikely to be stored in the form of gas, and the supercritical state has the greatest storage potential in the formation [10,11]. Gas reservoirs whose formation temperature and pressure exceed the critical point of CO<sub>2</sub> are the most suitable sites for CO<sub>2</sub> storage. Therefore, from the perspective of economic benefits, it is a hot research topic to achieve enhanced natural gas recovery by injecting CO<sub>2</sub> into gas reservoirs and using its own conditions for storage [12]. There are two schemes to reduce the concentration of carbon dioxide in the atmosphere. The first scheme focuses on reducing the emission of carbon dioxide into the air. The utilization of carbon dioxide mentioned in this paper can improve the oil recovery of tight sandstone gas reservoirs and increase the supply of natural gas, so that it can replace coal, oil and other resources with large carbon dioxide emissions and natural gas emissions under the same power generation conditions and reduce the emission of carbon dioxide into the air. At the same time, the carbon dioxide injected into the stratum is stored in the stratum, which can effectively treat the discharged carbon dioxide. In a functional coal-fired power plant, the 660 MWe supercritical coal-fired boiler is always based on traditional and advanced artificial intelligence, using technology to present comprehensive data visualization, and an effective and verified artificial neural network is developed. Compared with the least square support vector machine process model, the artificial neural network process model is proved to be obviously more effective and used for industrial data analysis and decision making. When the unit load is 50%, 75% and 100%, the heat input value can be reduced by 7.20%, 6.85% and 8.60%, respectively, without affecting the overall thermal efficiency of the power plant [13]. Negative emission technology can effectively remove carbon dioxide from the atmosphere. Common technologies include afforestation, forest management, vegetation restoration and other measures. Plant photosynthesis is used to absorb carbon dioxide from the atmosphere and fix it in vegetation and soil to reduce the concentration of carbon dioxide in the air. Capturing carbon dioxide in ivy plants growing on the external walls of houses is a quick supplementary way to achieve the global GHG emission reduction goal, which can help achieve the carbon dioxide emission reduction goal [14].

In China, there are many studies on enhanced oil recovery by carbon dioxide gas flooding in tight sandstone reservoirs in the existing literature. There are many factors that

affect the effect of CO<sub>2</sub> flooding, which are mainly divided into three categories: reservoir parameters, formation fluid properties and gas injection methods. Among them, reservoir parameters mainly include reservoir heterogeneity, reservoir thickness and permeability, and fluid properties mainly include crude oil viscosity and crude oil density. Formation heterogeneity, oil–gas viscosity ratio, formation sedimentation rhythm, miscible–immiscible, vertical and horizontal permeability ratio and development mode are the main factors affecting CO<sub>2</sub> displacement efficiency and storage coefficient. The permeability of the formation has little influence on CO<sub>2</sub> displacement efficiency and storage coefficient, but it has great influence on injection production speed and production time, such as low-permeability reservoirs, which is not conducive to the rapid storage of CO<sub>2</sub> [15]. This study draws lessons from the research results of CO<sub>2</sub> injection in tight sandstone reservoir to understand its influencing factors and makes targeted experiments to explore the mechanism of CO<sub>2</sub> injection in complex tight sandstone gas reservoirs to enhance oil recovery and burial.

The research results of carbon dioxide injection into other gas reservoirs outside China show that numerical simulation is used to evaluate the influence of the duration of carbon dioxide injection period on natural gas recovery during initial gas–water contact. The research shows that when carbon dioxide is injected, an artificial barrier is formed to partially block the formation water. The final gas recovery rate is 61.98% when carbon dioxide is injected and 48.04% when the reservoir is exhausted and developed. Injecting carbon dioxide to improve ultimate oil and gas recovery [16]. The efficiency of carbon dioxide injection technology is studied by numerical simulation to control the water injection process of the V-16 reservoir in the Hadiach oil and gas condensate field and to replace the residual natural gas reserves trapped by formation water. According to the calculation results, for the control of water injection process in production formation, the number of injection wells has a considerable impact on the efficiency of the analyzed technology, which provides a more complete coverage of gas-bearing areas with carbon dioxide, making the efficiency of preventing formation water from flowing into production wells higher. The research results show that compared with depleted oil and gas field development, the predicted natural gas recovery increased by 2.95% and condensate recovery increased by 1.24% [17]. Injecting carbon dioxide into gas reservoirs can greatly improve gas reservoir recovery.

Some research results have been achieved on the implementation of CO<sub>2</sub> storage in natural gas reservoirs and the use of supercritical CO<sub>2</sub> to enhance natural gas recovery [18]. Some researchers have carried out basic research on CO<sub>2</sub> enhanced recovery and storage technology and simplified natural gas into pure CH<sub>4</sub> [19]. When the temperature and pressure of gas reservoirs with a depth of more than 800 m exceed the CO<sub>2</sub> critical point, CO<sub>2</sub> can be in a supercritical state and exists underground, and at the same time, its supercritical density is higher than that of natural gas, close to liquid, with a certain strength; the diffusion coefficient is close to that of gas, about 100 times that of liquid; and it has good fluidity. Some researchers use CO<sub>2</sub> storage to increase oil and gas recovery, mainly by injecting CO<sub>2</sub> into production wells to displace oil or gas [20]. It has been proved that CO<sub>2</sub> displacement technology can prolong the life of oilfields by at least 20 years. Combined with oil displacement technology, it greatly improves the profit of mining [21,22]. Some researchers have studied the potential of gas injection to enhance oil recovery in major oil areas in China. The 17 oil areas suitable for CO<sub>2</sub> miscible displacement have  $1.6 \times 10^8$  t of geological reserves, accounting for 10.4% of the total reserves. The enhanced oil recovery rate is 16.4%, and the recoverable reserves are increased by  $1.7 \times 10^8$  t. At the same time, it proves that China's oil reservoirs have considerable potential for CO<sub>2</sub> geological storage [23]. Some researchers take long core as the research object and, through indoor experiments and numerical simulation methods, inject supercritical CO<sub>2</sub> into the condensate gas reservoir circularly to obtain higher condensate oil recovery and obtain a large number of components [24]. This is mainly due to the reverse evaporation of heavy components into the CO<sub>2</sub> condensate gas mixture caused by thermal gradient. With the increase in temperature, the formation fluid flow rate increases, which increases the gas

phase viscosity and decreases the liquid phase viscosity, promotes the thermal diffusion, increases the dissolution effect of CO<sub>2</sub> and enhances the reverse evaporation intensity to improve its recovery [25]. Some researchers have studied the cyclic gas injection test in the fractured gas reservoir. By injecting different gases into a fractured core and conducting long core physical simulation experiments, they found that the injection timing and the composition of injected gas are two key parameters to achieve miscible gas [26–28]. The miscible gas injected into the condensate gas reservoir has obtained greater condensate recovery. At the same time, the existence of a fracture system near the matrix is more conducive to the depletion of pressure in the matrix and the recovery of more condensate. When injecting gas under miscible and immiscible pressures, it can be observed that the higher the injection pressure and the lower the condensate content in the matrix core, the greater the condensate recovery [29].

The research outside China is mainly concentrated in North America. Using CO<sub>2</sub> to enhance oil recovery is an effective way to realize CO<sub>2</sub> storage in depleted oil and gas reservoirs.

In 2008, the output of CO<sub>2</sub>-EOR in the world was  $27.25 \times 10^4$  barrels per day, and that in the United States was  $24.79 \times 10^4$  barrels per day, accounting for 91% of the daily output of CO<sub>2</sub>-EOR in the world, and the number of projects accounted for 85% of the world. CO<sub>2</sub> flooding includes miscible flooding, immiscible flooding and injection. CO<sub>2</sub> injection can improve oil recovery by 8~15%. The most widely used EOR technology in the world is located in North America, and the United States has mature CO<sub>2</sub>-EOR technology. IEA predicted in 2008 that the potential of CO<sub>2</sub>-EOR in the world is  $1600 \times 10^8 \sim 3000 \times 10^8$  barrels, which is equivalent to 7~14% of the current recoverable crude oil in the world [30].

At present, the research of carbon dioxide gas flooding in complex tight sandstone gas reservoirs is still blank. This paper verifies the influencing factors of carbon dioxide displacement on core tight gas recovery through core displacement experiments, which provides a reliable basis for the popularization and application of this technology.

The complex tight sandstone has the characteristics of low porosity, low permeability and a large area of concealed gas reservoirs [31,32]. By injecting CO<sub>2</sub> into the formation, the recovery rate of natural gas can be improved, and the stable storage of CO<sub>2</sub> can be achieved at the same time [33]. In this paper, taking the complex and tight sandstone of the Upper Paleozoic in the Ordos Basin as the research object, through laboratory physical simulation experiments, the effects of displacement rate, fissure dip, core permeability, core dry and wet on CO<sub>2</sub> displacement efficiency and storage efficiency were carried out [34]. The effects of different factors on CO<sub>2</sub> displacing efficiency and storage efficiency are analyzed, which provides theoretical data support for CO<sub>2</sub> injection in complex tight sandstone gas reservoirs to improve recovery and storage efficiency [35].

The main purpose of this paper is to provide experimental basis for carbon dioxide displacement development of complex tight sandstone gas reservoirs in the later stage through carbon dioxide core displacement experiments and at the same time provide necessary experimental parameters for permanent carbon sequestration of carbon-dioxide-depleted oil and gas reservoirs, so as to improve gas reservoir recovery and carbon sequestration.

## 2. Experimental Methods

### 2.1. Geological Background of the Study Area

The Ordos Basin is located in the west-central part of China. The basin is generally rhombus-shaped, extending from north to south. It is adjacent to Yinshan and Daqingshan in the north, Qinling Mountains in the south, Luliang Mountain in the east and Liupan Mountain in the west. This paper selects the tight sandstone reservoirs in the Hangjinqi area of the Ordos Basin. The recoverable positions of natural gas in the study area are Carboniferous and Permian, including the Lower Shihezi Formation, Upper Shihezi Formation and Shiqianfeng Formation. Table 1 shows the specific characteristics of each stratum in the study area. The lithology of the Lower Shihezi Formation and Upper Shihezi Formation are relatively diverse, and the coal seams and mudstones have strong hydrocarbon

generation capacity, providing good source rock conditions for the formation of natural gas reservoirs in this area. Sandstone and glutenite developed in the Shiqianfeng Formation have relatively good reservoir properties, providing good reservoir conditions and good cap rock conditions for gas accumulation.

**Table 1.** Characteristics of each stratum in the study area.

Stratum Name	Stratigraphic Characteristics
Lower Shihezi Formation	It is widely distributed on the plane and basically distributed in the whole study area. It is composed of He1 Member, He2 Member and He3 Member longitudinally. The lithology is mainly sandstone, with a certain amount of mudstone mixed between them. The reservoir physical property of Xiahezi Formation sandstone is the best, and it is the most important reservoir in this area.
Upper Shihezi Formation	It is widely distributed on the plane. The lithology is sandstone and mudstone. The thickness of mudstone is relatively large, with a total thickness of more than 100 m. It has good capping capacity, providing good capping conditions for natural gas accumulation.
Shiqianfeng Formation	The whole area is distributed on the plane, and the lithology is dominated by sandstone and mudstone. As a regional caprock, mudstone is thicker and has stronger sealing capacity.

## 2.2. Experimental Scheme

In this paper, cores with different physical properties of tight sandstone gas reservoirs are used to simulate the reservoir conditions according to the temperature, pressure and formation fluid composition of tight gas reservoirs. The cores are filled with natural gas and injected with carbon dioxide at different injection rates and angles. The experiments are divided into 10 groups, and the effects of various factors on CO<sub>2</sub> displacement efficiency and storage efficiency are studied through the experimental results of different groups.

The tight sandstone cores in the study area are selected and divided into 10 groups of CO<sub>2</sub> displacement CH<sub>4</sub> experiments. The displacement velocities are set as 0.1 mL/min, 0.2 mL/min, 0.4 mL/min and 0.8 mL/min, respectively. The injection end dip angles are 45°, −10°, −45° and nearly horizontal. For cores with low, medium and high permeability, the permeability, respectively, is  $2.18 \times 10^{-3} \mu\text{m}^2$ ,  $9.66 \times 10^{-3} \mu\text{m}^2$  and  $1.03 \times 10^{-3} \mu\text{m}^2$ , and the influence group whether there is bound water is set up. The influence of core permeability, gas injection rate, the existence of formation water and gravity on the gas displacement efficiency and storage efficiency when CO<sub>2</sub> displaces CH<sub>4</sub> are studied, and the diffusion degree of CO<sub>2</sub>-CH<sub>4</sub> under different influence factors is evaluated. Table 2 shows the experimental schemes for different cores.

**Table 2.** Experimental scheme of different cores.

Experiment Order	Influencing Factors	Experimental Content
1	Displacement Speed	0.1 mL/min horizontal displacement of medium-seepage dry core
2		0.2 mL/min horizontal displacement of dry cores with medium permeability
3		0.4 mL/min horizontal displacement of dry cores with medium permeability
4		0.8 mL/min horizontal displacement of medium-seepage dry core
5	Inclination	0.2 mL/min, inlet +45° displacement medium-seepage dry core
6		0.2 mL/min, inlet −10° displacement medium-seepage dry core
7		0.2 mL/min, inlet −45° displacement medium-seepage dry core
8	Penetration	0.2 mL/min horizontal displacement of low-seepage dry core
9		0.2 mL/min horizontal displacement of high-seepage dry core
10	Bound water	0.2 mL/min displacement of medium-seepage cores with bound water

In the experiment, the core displacement equipment of RUSKA Company in the United States was used, mainly including an injection system, a core-clamping system and a recovery system. The auxiliary equipment mainly includes a constant-pressure and



constant-speed displacement pump, a gas meter and a gas chromatograph. According to the displacement mechanism and similarity principle, automatic core oil displacement device simulates formation pressure and temperature conditions and carries out various simulation tests on cores with the help of modern science and technology. We can study the seepage characteristics of a simulated oil displacement system in porous media (liquid permeability, oil–water relative permeability, basic water injection experiment) and the influence of oil displacement efficiency. It can be used to study oil production technology, such as fracturing, water plugging, adjusting the injection–production profile and so on. The device is a comprehensive device, including water flooding, chemical flooding, CO<sub>2</sub> gas flooding and N<sub>2</sub> gas flooding, which can simulate the flow of various oil displacement systems. The annular pressure tracks the injection pressure of the gripper and maintains a constant differential pressure. With manual, electric, constant pressure, tracking functions, etc. The model temperature is adjustable and controllable and can be heated and controlled according to the program setting. Automatic switching of pressure sensors takes place with different ranges.

Table 3 shows the composition of formation water samples in the experiment, mainly including industrial high-purity CO<sub>2</sub> (molar concentration > 99.9%) and high-purity CH<sub>4</sub> (molar concentration > 99%). The formation water is prepared according to the ion content and salinity of the on-site formation water.

**Table 3.** Composition of formation water samples in the experiment.

K <sup>+</sup> + Na <sup>+</sup>	Mg <sup>2+</sup>	Ca <sup>2+</sup>	Cl <sup>−</sup>	SO <sub>4</sub> <sup>2−</sup>	HCO <sub>3</sub> <sup>−</sup>	CO <sub>3</sub> <sup>2−</sup>	Total Salinity (mg/L)
12,170	26	31	17,380	270	2431	0	32,308

All cores in the experiment are divided into three groups. Formation sampling and artificial cores are divided into relatively high permeability, medium permeability and low permeability. At present, the drilling core technology is limited, and it is impossible to directly obtain cores with a length of 1 m. During the experimental test, the temperature is realized by multiple sets of heating plates in the incubator, and the pressure is monitored by the measured electronic pressure gauge. The high-pressure corrosion-resistant rubber sleeve is installed in the core holder for sealing. Table 4 shows the physical parameter information table of low-permeability cores, and the cores are sorted from exit to entry and from top to bottom.

**Table 4.** Low-permeability core physical parameter information table.

Core Number	Core Length (cm)	Core Diameter (cm)	Pore Volume (cm <sup>3</sup> )	Porosity (%)	Permeability (10 <sup>−3</sup> μm <sup>2</sup> )
1	4.31	2.51	2.35	11.2	1.8
2	4.84	2.56	2.73	11.0	1.8
3	5.11	2.49	2.85	11.3	2.3
4	5.23	2.51	2.91	11.4	2.4
5	5.32	2.49	2.83	11.0	2.3
6	4.53	2.53	2.51	11.4	1.9
7	4.64	2.48	2.83	11.2	1.9
8	5.01	2.56	2.75	11.4	2.6
9	5.32	2.56	2.82	11.1	2.1
10	5.21	2.53	2.84	11.3	2.0

### 2.3. Experimental Conditions and Steps

In the experiment, the core temperature is set to 80 °C, the pressure is set to 8 MPa (controlled back pressure) and constant speed displacement is adopted. The experimental steps are:

- (1) Put the short core into the long-core holder in sequence, put it into the thermostat according to the angle of the injection end and connect the displacement device;
- (2) Add 10 MPa confining pressure to the core, limit the maximum pressure to 5 MPa at the speed of 5 mL/min through the advection pump and use the mixture of displacing

petroleum ether and anhydrous ethanol to clean the long core until the outlet fluid is free of discoloration and impurities;

(3) Use nitrogen to drive long core at 2 MPa constant pressure for 12 h, and vacuum the long core after drying for 5 h;

(4) Fill saturated high-purity  $\text{CH}_4$  gas, increase the core confining pressure to 12 MPa, use constant pressure 8 MPa to saturate  $\text{CH}_4$  and close the outlet valve port; when the inlet pressure reaches 8 MPa and is maintained for 4 h,  $\text{CH}_4$  saturation can be considered as complete;

(5) Connect the high-purity  $\text{CO}_2$  intermediate container, drive  $\text{CH}_4$  in the core at the design speed, set the back pressure to 8 MPa, record the gas volume every 0.1 PV and test the composition of the produced gas; use a gas chromatograph to analyze  $\text{CH}_4$  and  $\text{CO}_2$  content to calculate  $\text{CH}_4$  recovery rate; when the  $\text{CO}_2$  content reaches more than 98% or the  $\text{CH}_4$  recovery rate no longer increases, the displacement is stopped and the experiment is completed;

(6) After the experiment, vacuum the core again and saturate  $\text{CH}_4$  to conduct the next group of displacement experiments;

(7) By changing the angle of long-core gripper, high injection low production or low injection high production with different dip angles can be realized.

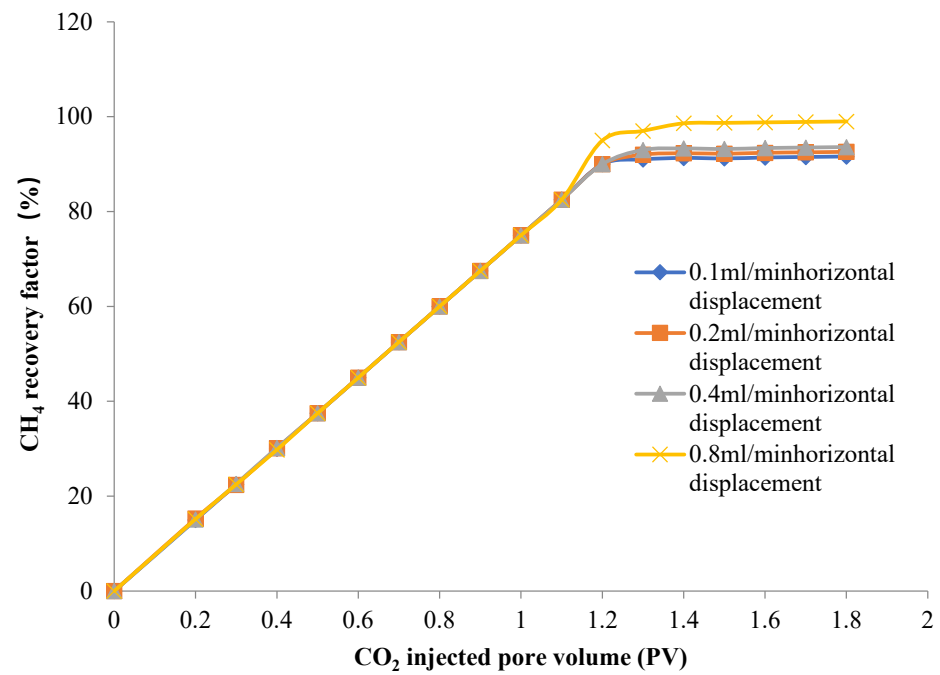
### 3. Experimental Results and Analysis

#### *Test Results*

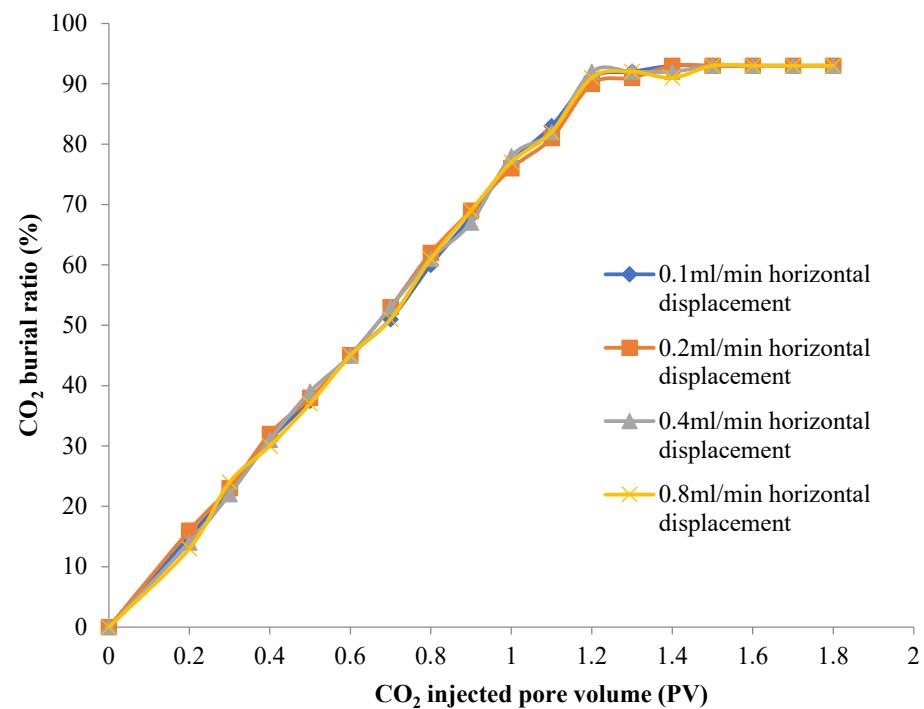
According to the designed experimental scheme, the experiments were carried out under the conditions of 80 °C and 8 MPa with  $\text{CO}_2$  displacement rates of 0.1 mL/min, 0.2 mL/min, 0.4 mL/min and 0.8 mL/min on the permeability of saturated high-purity  $\text{CH}_4$ . The cores were displaced, and the effects of different displacement rates, different dip angles, different permeability cores and dry and wet cores on  $\text{CO}_2$  storage efficiency were analyzed.

Figure 1 shows the change of core  $\text{CH}_4$  recovery with  $\text{CO}_2$  injection pore volume under different displacement velocities. It can be seen from Figure 1 that when the  $\text{CO}_2$  injected pore volume is less than 1 PV, the relationship between the  $\text{CH}_4$  recovery factor and the  $\text{CO}_2$  injected pore volume is linearly correlated, and the inclination angle is 45°; when the  $\text{CO}_2$  injected pore volume exceeds 1 PV, the recovery factor of  $\text{CH}_4$  increases slightly with the increase in displacement speed; when the displacement rate is 0.8 mL/min, compared with the displacement rate of 0.1 mL/min,  $\text{CH}_4$  recovery is about 8% higher. The results show that diffusion occurs at the front of displacement, and the mixing time of  $\text{CO}_2$  and  $\text{CH}_4$  in porous media increases during low-speed displacement, which is easy to form a wider miscible zone, resulting in lower  $\text{CH}_4$  recovery when  $\text{CO}_2$  breaks through, but the final recovery is not much different.

The  $\text{CO}_2$  storage rate refers to the ratio of the  $\text{CO}_2$  storage amount to the core pore volume, and the  $\text{CO}_2$  storage ratio refers to the ratio of the  $\text{CO}_2$  storage amount to the total amount of  $\text{CO}_2$  injected. The  $\text{CO}_2$  storage efficiency under different experimental conditions was studied by calculating the  $\text{CO}_2$  storage rate and storage ratio. Figure 2 shows the relationship between the  $\text{CO}_2$  storage rate of the core and the injected pore volume under different displacement rates. It can be seen from Figure 2 that before  $\text{CO}_2$  breakthrough, the  $\text{CO}_2$  storage efficiency increases in a 45° oblique line. After the  $\text{CO}_2$  breakthrough, the smaller displacement rate makes the  $\text{CO}_2$  storage rate increase slowly, which indicates that the mixing time of  $\text{CO}_2$  front and  $\text{CH}_4$  is longer, and the transition zone is wider. With the  $\text{CO}_2$  breakthrough, the  $\text{CO}_2$  storage rate decreases, and the final  $\text{CO}_2$  storage rate under different displacement rates is consistent. Figure 3 shows the relationship between the  $\text{CO}_2$  storage ratio and the injected pore volume in the core under different displacement rates. It can be seen from Figure 3 that with the continuous injection of  $\text{CO}_2$ , the initial storage ratio of  $\text{CO}_2$  is 100%, but with the  $\text{CO}_2$  breakthrough, the storage ratio will gradually decrease. When the  $\text{CO}_2$  injection exceeds 1 PV, under the same PV number, the rate of  $\text{CO}_2$  storage at different displacement speeds is basically consistent.



**Figure 1.** CH<sub>4</sub> recovery of cores with different displacement velocities varies with the pore volume of CO<sub>2</sub> injection.



**Figure 2.** CO<sub>2</sub> storage efficiency in cores under different displacement rates.



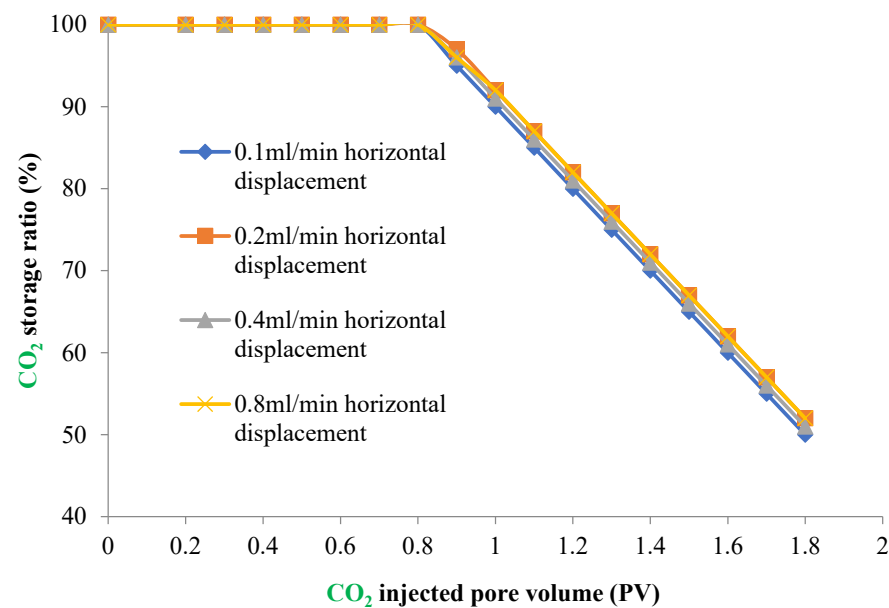


**Figure 3.** CO<sub>2</sub> storage ratio in cores under different displacement rates.

Figure 4 shows the relationship between CH<sub>4</sub> recovery rate of core and CO<sub>2</sub> injection pore volume under different displacement angles. It can be seen from Figure 4 that the CH<sub>4</sub> recovery factor is linearly related to the injected pore volume, and the inclination angle is 45°. At the same time, when CO<sub>2</sub> breakthrough occurs, the CH<sub>4</sub> recovery factor (76%) of high injection and low recovery is 11% lower than that of low injection and high recovery. The higher the outlet end is, the greater the recovery factor will be. The results show that under the action of gravity, gravity affects the breakthrough time of CO<sub>2</sub>. When CO<sub>2</sub> is injected from a high position, the width of the transition zone is increased, the breakthrough is advanced and the recovery of CH<sub>4</sub> is reduced.

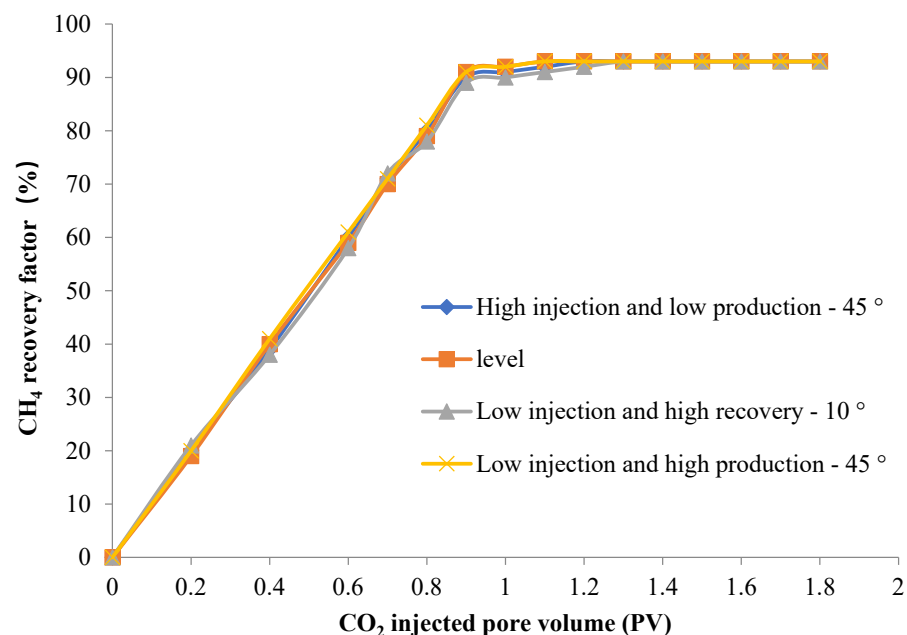


**Figure 4.** CH<sub>4</sub> recovery of cores with different displacement velocities varies with the pore volume of CO<sub>2</sub> injection.

Figure 5 shows the relationship between CO<sub>2</sub> storage rate and injected pore volume in cores under different displacement angles. It can be seen from Figure 5 that before the CO<sub>2</sub> breakthrough, the CO<sub>2</sub> storage rate increases in a 45° oblique straight line. After the CO<sub>2</sub>

breakthrough, the growth rate of CO<sub>2</sub> storage rate slows down. At the same time, because the breakthrough of high injection and low production is earlier, the final CO<sub>2</sub> storage rate is lower than that of horizontal displacement and low injection and high production. The research results show that the mixing transition zone of CO<sub>2</sub> and CH<sub>4</sub> is wider due to gravity when displacing in high position. When CO<sub>2</sub> breaks through, the CO<sub>2</sub> will increase with CH<sub>4</sub> production, which will lead to a decrease in the storage rate. The higher the outlet end, the greater the CO<sub>2</sub> storage rate will be.

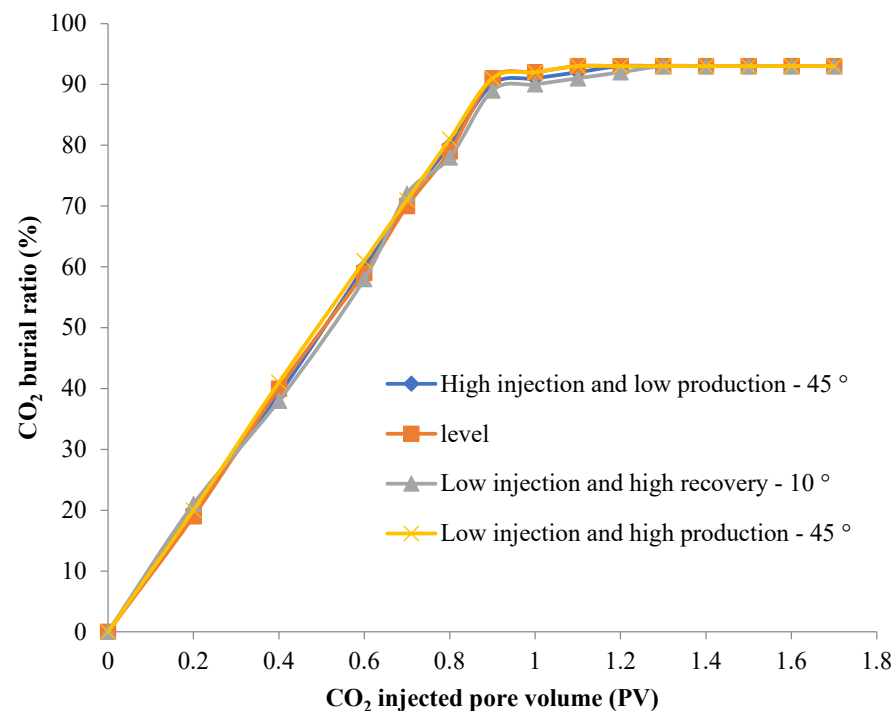


**Figure 5.** CO<sub>2</sub> storage efficiency in cores under different displacement angles.

Figure 6 shows the relationship between the buried proportion of CO<sub>2</sub> in the core and the injected pore volume under different displacement velocities. It can be seen from Figure 6 that with the continuous injection of CO<sub>2</sub>, the storage ratio of CO<sub>2</sub> at the initial stage is 100%, but after the breakthrough of CO<sub>2</sub>, the storage ratio of CO<sub>2</sub> will gradually decrease. After the injection exceeds 1 PV, the storage ratio of CO<sub>2</sub> at different displacement angles is about 93%.

Figure 7 shows the relationship between CH<sub>4</sub> recovery factor and CO<sub>2</sub> injection pore volume of cores with different permeability under the same injection conditions. It can be seen from Figure 7 that before CO<sub>2</sub> breakthrough, the CH<sub>4</sub> recovery rate is linearly related to the injected pore volume, with an inclination of 45°; after CO<sub>2</sub> breakthrough, with the increase in core permeability, the recovery factor of CH<sub>4</sub> is higher. The research results show that in the low-permeability core, the diffusion of CO<sub>2</sub> is stronger, the transition zone between CO<sub>2</sub> and CH<sub>4</sub> is larger and the produced CH<sub>4</sub> is polluted, thus reducing the recovery factor.

Figure 8 shows the relationship between CO<sub>2</sub> storage rate and injected pore volume in cores with different permeability. It can be seen from Figure 8 that before CO<sub>2</sub> breakthrough, the CO<sub>2</sub> storage rate increases in a 45° oblique straight line; after CO<sub>2</sub> breakthrough, the CO<sub>2</sub> storage rate increases slowly. With the increase in core permeability, the CO<sub>2</sub> storage rate increases. Figure 9 shows the relationship between CO<sub>2</sub> storage ratio of cores with different permeability and injected pore volume. It can be seen from Figure 9 that with the increase in permeability, the CO<sub>2</sub> storage effect of the core is better. The results show that the diffusion of CO<sub>2</sub> is stronger in low-permeability cores, and the process of displacement of CH<sub>4</sub> by CO<sub>2</sub> tends to piston displacement with higher permeability.

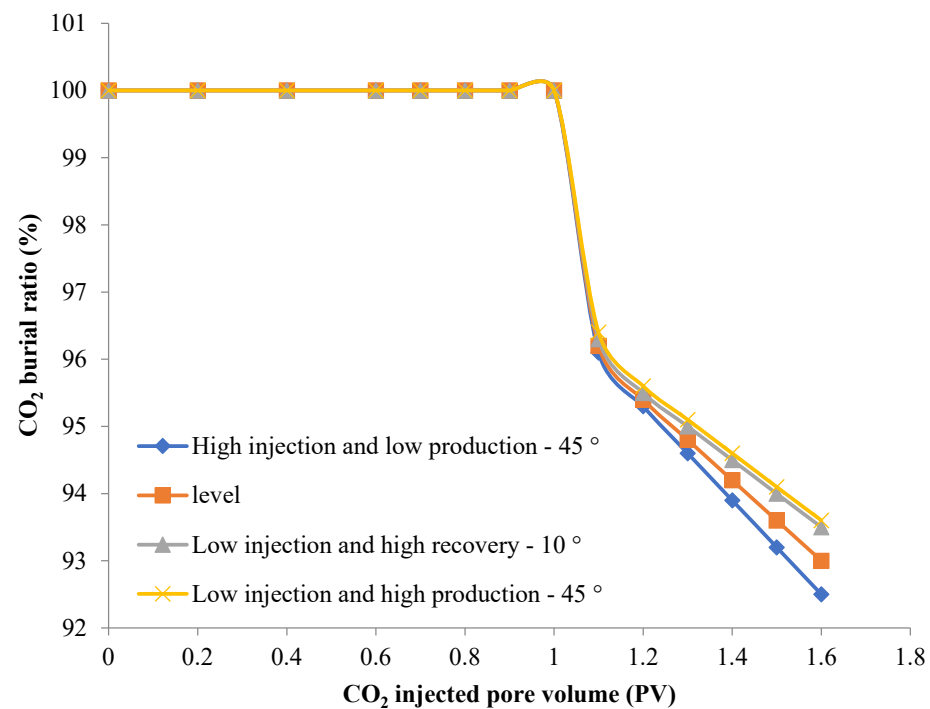


Figure 6. CO<sub>2</sub> storage ratio in cores under different displacement angles.

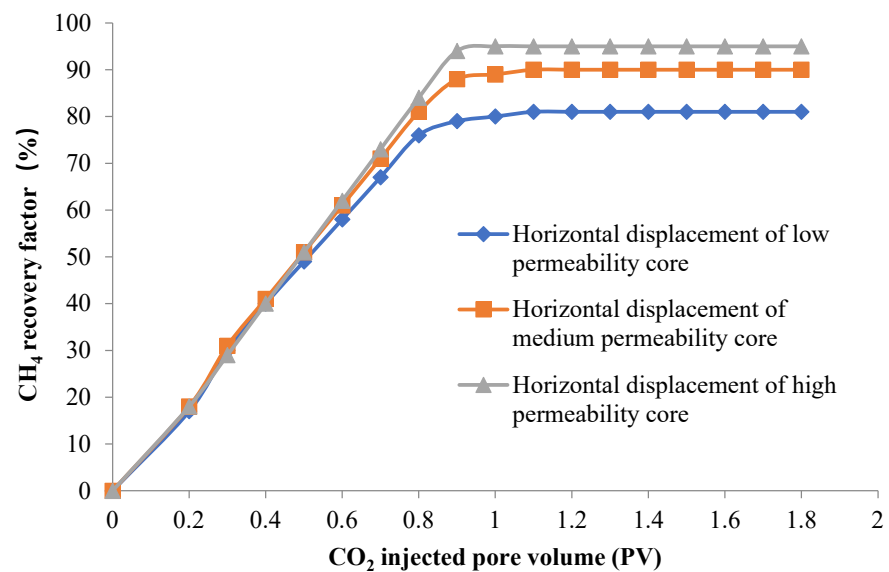


Figure 7. CH<sub>4</sub> recovery factor with CO<sub>2</sub> injection pore volume in cores with different permeability.

According to the relationship between the recovery of CH<sub>4</sub> in dry and wet cores and the injected pore volume, when bound water exists, there is little CO<sub>2</sub> effectively displaced in the initial stage of wet-core injection. When the bound water dissolves CO<sub>2</sub> to saturation, CH<sub>4</sub> is effectively displaced, so the recovery of CH<sub>4</sub> lags behind; at the same time, the existence of bound water makes the micropores in the core mainly filled with water, and CH<sub>4</sub> is more likely to be displaced by CO<sub>2</sub>, making the CH<sub>4</sub> recovery of the final wet core slightly higher than that of the dry core.

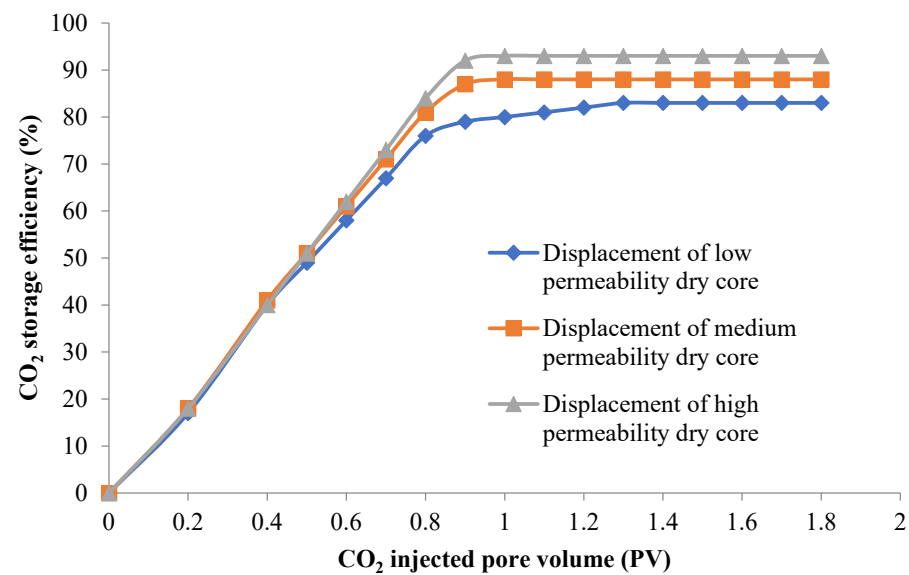


Figure 8. CO<sub>2</sub> storage efficiency in cores with different permeability.

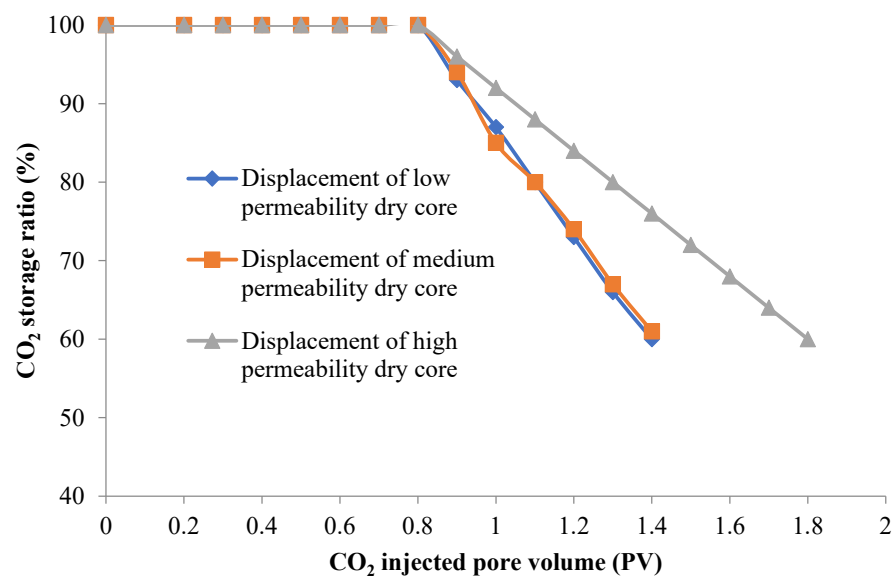


Figure 9. CO<sub>2</sub> storage ratio in cores with different permeability.

According to the relationship between the CO<sub>2</sub> storage rate and storage ratio of dry and wet cores and the pore volume of CO<sub>2</sub> injection, when bound water is not considered in the core, when 1.4 PV~1.6 PV of CO<sub>2</sub> is injected, the retention ratio is about 60%; in the presence of bound water, the CO<sub>2</sub> retention rate increases significantly at the same injection of PV, which fully shows that the existence of formation water is conducive to the storage of CO<sub>2</sub> in the ground; at the same time, after storage, the underground saturation of CO<sub>2</sub> is consistent with the degree of CH<sub>4</sub> production, it indicates that CO<sub>2</sub> occupies a certain space. In addition to occupying the space of the displaced CH<sub>4</sub>, a small part of CO<sub>2</sub> is also dissolved in the formation water when the bound water exists. The dissolved CO<sub>2</sub> accounted for about 1.89% of the pore volume under the conditions of 8 Mpa and 80 °C, and the higher the pressure, the larger the dissolved amount.

CO<sub>2</sub> displacing CH<sub>4</sub> can effectively improve oil recovery and realize geological storage of CO<sub>2</sub> in gas reservoirs. The overall recovery ratio of CO<sub>2</sub> displacing CH<sub>4</sub> is 87–97%, and the breakthrough time of CO<sub>2</sub> is 0.7–0.9 PV. When CO<sub>2</sub> breaks through, CH<sub>4</sub> recovery is 72–88%. When 1.5–2.4 PV is injected, the CO<sub>2</sub> storage rate is about 50%. When CO<sub>2</sub>

occupies CH<sub>4</sub> space in the reservoir and bound water exists, the saturation of CO<sub>2</sub> in the reservoir is about 55%, and the part dissolved in water accounts for 1.9% PV.

The diffusion of CO<sub>2</sub> molecules is more significant in low-permeability and low-velocity displacement cores. When the displacement speed is lower, the breakthrough time of CO<sub>2</sub> is earlier. With the increase in displacement speed, the final recovery rate of CH<sub>4</sub> increases slightly. When the permeability is lower, the breakthrough time of CO<sub>2</sub> is earlier when PV is injected at the same time, and the final CH<sub>4</sub> recovery rate is lower. Under the action of gravity, it has a great influence on CO<sub>2</sub> storage and enhanced oil recovery. The breakthrough of CO<sub>2</sub> with high injection and low production is earlier, the transition zone takes longer and the CH<sub>4</sub> recovery is about 3.3% lower than that with low injection and high production.

The dissolution of CO<sub>2</sub> in formation water affects the breakthrough time and recovery ratio of CO<sub>2</sub> displacing CH<sub>4</sub>. When bound water exists, the displacement-phase CO<sub>2</sub> is partially dissolved in formation water, and the breakthrough of CO<sub>2</sub> lags behind about 0.1 PV, and the final CH<sub>4</sub> recovery ratio and CO<sub>2</sub> storage ratio are higher than that of dry-core displacement.

#### 4. Conclusions

With the popularization of natural gas and the requirements of environmental protection, the development and utilization of natural gas is particularly important. The Upper Paleozoic tight sandstone in the Ordos Basin has the characteristics of low porosity, low permeability and concealed gas reservoir. By injecting CO<sub>2</sub> into the formation, the recovery rate of natural gas can be effectively improved, and the stable storage of CO<sub>2</sub> can be realized. This paper takes the complex and tight sandstone of the Upper Paleozoic in the Ordos Basin as the research object. Through laboratory experiments, the effects of displacement rate, fracture dip angle, core permeability, and core dry and wet on CO<sub>2</sub> displacement efficiency and storage efficiency are analyzed. The influence of these factors on CO<sub>2</sub> displacement and storage efficiency thus improves CH<sub>4</sub> recovery and CO<sub>2</sub> storage efficiency. The main research results are:

(1) For different cores, when the CO<sub>2</sub> injection pore volume is lower than 1 PV, the relationship between CH<sub>4</sub> recovery factor and CO<sub>2</sub> injection pore volume is linear, and the inclination angle is 45°. When the CO<sub>2</sub> injection pore volume exceeds 1 PV, the CH<sub>4</sub> recovery factor increases slightly with the increase in displacement speed. Before CO<sub>2</sub> breakthrough, the CO<sub>2</sub> storage efficiency increases in a 45° oblique straight line. After CO<sub>2</sub> breakthrough, the CO<sub>2</sub> storage rate increases slowly. After CO<sub>2</sub> breakthrough, the CO<sub>2</sub> storage rate decreases, and the final CO<sub>2</sub> storage rate is consistent. With the continuous injection of CO<sub>2</sub>, the stored proportion of CO<sub>2</sub> in the initial stage is 100%, but when CO<sub>2</sub> breaks through, the stored proportion will gradually decrease. When CO<sub>2</sub> injection exceeds 1 PV, the stored proportion of CO<sub>2</sub> under the same PV number is basically the same.

(2) The recovery rate of CH<sub>4</sub> displaced by CO<sub>2</sub> is generally 87–97%, and the CO<sub>2</sub> breakthrough time is 0.7–0.9 PV. After 2.4 PV, the CO<sub>2</sub> storage rate is basically about 50%; when 1.5–2.4 PV is injected, the CO<sub>2</sub> storage rate is basically about 50%, and the CO<sub>2</sub> saturation in the reservoir is about 55% when there is bound water. The water part accounts for 1.9% PV; when the displacement rate is lower, the breakthrough time of CO<sub>2</sub> is earlier; with the increase in the displacement rate, the final recovery rate of CH<sub>4</sub> increases slightly; when the permeability is lower, under the same injection of PV, the CO<sub>2</sub> breakthrough time is earlier, and the final CH<sub>4</sub> recovery rate is lower; when the bound water exists, the displacement-phase CO<sub>2</sub> is partially dissolved into the formation water, the CO<sub>2</sub> breakthrough lag is about 0.1 PV, and the final CH<sub>4</sub> recovery rate and CO<sub>2</sub> storage rate are higher than that of dry-core displacement.

(3) Other conditions being unchanged, the higher the core permeability, the higher the CH<sub>4</sub> recovery rate and the higher the CO<sub>2</sub> storage rate.



**Author Contributions:** Conceptualization, L.Z.; methodology, H.C.; formal analysis, Z.L.; writing—original draft preparation, H.C.; writing—review and editing, Z.L.; supervision, Q.Z.; project administration, X.Z.; funding acquisition, T.B. All authors have read and agreed to the published version of the manuscript.

**Funding:** This research received no external funding.

**Data Availability Statement:** The figures and tables used to support the findings of this study are included in the article.

**Acknowledgments:** The authors would like to show sincere thanks to those techniques who have contributed to this research.

**Conflicts of Interest:** The authors declare no conflict of interest.

## References

1. Wu, S.; Zou, C.; Ma, D.; Zhai, X.; Yu, H.; Yu, Z. Reservoir property changes during CO<sub>2</sub>–brine flow-through experiments in tight sandstone: Implications for CO<sub>2</sub> enhanced oil recovery in the Triassic Chang 7 Member tight sandstone, Ordos Basin, China. *J. Asian Earth Sci.* **2019**, *179*, 200–210. [\[CrossRef\]](#)
2. Jin, L.; Hawthorne, S.; Sorensen, J.; Pekot, L.; Kurz, B.; Smith, S.; Heebink, L.; Herdegen, V.; Bosshart, N.; Torres, J.; et al. Advancing CO<sub>2</sub> enhanced oil recovery and storage in unconventional oil play—Experimental studies on Bakken shales. *Appl. Energy* **2017**, *208*, 171–183. [\[CrossRef\]](#)
3. Zhou, X.; Wang, Y.; Zhang, L.; Zhang, K.; Jiang, Q.; Pu, H.; Wang, L.; Yuan, Q. Evaluation of enhanced oil recovery potential using gas/water flooding in a tight oil reservoir. *Fuel* **2020**, *272*, 117706. [\[CrossRef\]](#)
4. Li, D.; Saraji, S.; Jiao, Z.; Zhang, Y. CO<sub>2</sub> injection strategies for enhanced oil recovery and geological storage in a tight reservoir: An experimental study. *Fuel* **2021**, *284*, 119013. [\[CrossRef\]](#)
5. O'Brien, G.; Gunn, R.; Raistrick, M.; Buffin, A.; Tingate, P.; Miranda, J.; Arian, N. Victorian carbon dioxide geological storage options; an engineering evaluation of storage potential in southeastern Australia. *Energy Procedia* **2011**, *4*, 4739–4746. [\[CrossRef\]](#)
6. Burrows, L.C.; Haeri, F.; Cvetic, P.; Sanguinito, S.; Shi, F.; Tapriyal, D.; Goodman, A.L.; Enick, R.M. A literature review of CO<sub>2</sub>, natural gas, and water-based fluids for enhanced oil recovery in unconventional reservoirs. *Energy Fuels* **2020**, *34*, 5331–5380. [\[CrossRef\]](#)
7. Wang, L.; Tian, Y.; Yu, X.; Wang, C.; Yao, B.; Wang, S.; Winterfeld, P.H.; Wang, X.; Yang, Z.; Wang, Y.; et al. Advances in improved/enhanced oil recovery technologies for tight and shale reservoirs. *Fuel* **2017**, *210*, 425–445. [\[CrossRef\]](#)
8. Zhu, C.F.; Guo, W.; Wang, Y.P.; Li, Y.J.; Gong, H.J.; Xu, L.; Dong, M.Z. Experimental study of enhanced oil recovery by CO<sub>2</sub> huff-n-puff in shales and tight sandstones with fractures. *Pet. Sci.* **2021**, *18*, 852–869. [\[CrossRef\]](#)
9. AlRassas, A.M.; Vo Thanh, H.; Ren, S.; Sun, R.; Al-Areeq, N.M.; Kolawole, O.; Hakimi, M.H. CO<sub>2</sub> Storage and Enhanced Oil Recovery via the Water Alternating Gas Scheme in a Mixed Transgressive Sandstone-Carbonate Reservoir: Case Study of a Large Middle East Oilfield. *Energy Fuels* **2022**, *36*, 10299–10314. [\[CrossRef\]](#)
10. Chaturvedi, K.R.; Sharma, T. In-situ formulation of pickering CO<sub>2</sub> foam for enhanced oil recovery and improved carbon storage in sandstone formation. *Chem. Eng. Sci.* **2021**, *235*, 116484. [\[CrossRef\]](#)
11. Wang, Y.; Shang, Q.; Zhou, L.; Jiao, Z. Utilizing macroscopic areal permeability heterogeneity to enhance the effect of CO<sub>2</sub> flooding in tight sandstone reservoirs in the Ordos Basin. *J. Pet. Sci. Eng.* **2021**, *196*, 107633. [\[CrossRef\]](#)
12. He, Y.; Qiao, Y.; Qin, J.; Tang, Y.; Wang, Y.; Chai, Z. A novel method to enhance oil recovery by inter-fracture injection and production through the same multi-fractured horizontal well. *J. Energy Resour. Technol.* **2022**, *144*, 043005. [\[CrossRef\]](#)
13. Muhammad Ashraf, W.; Moeen Uddin, G.; Muhammad Arafat, S.; Afghan, S.; Hassan Kamal, A.; Asim, M.; Haider Khan, M.; Waqas Rafique, M.; Naumann, U.; Niazi, S.G.; et al. Optimization of a 660 MWe Supercritical Power Plant Performance—A Case of Industry 4.0 in the Data-Driven Operational Management Part 1. Thermal Efficiency. *Energies* **2020**, *13*, 5592. [\[CrossRef\]](#)
14. Krzywanski, J.; Ashraf, W.M.; Czakiert, T.; Sosnowski, M.; Grabowska, K.; Zylka, A.; Kulakowska, A.; Skrobek, D.; Mistal, S.; Gao, Y. CO<sub>2</sub> Capture by Virgin Ivy Plants Growing Up on the External Covers of Houses as a Rapid Complementary Route to Achieve Global GHG Reduction Targets. *Energies* **2022**, *15*, 1683. [\[CrossRef\]](#)
15. Liu, B.; Wang, C.; Zhang, J.; Xiao, S.; Zhang, Z.; Shen, Y.; Sun, B.; He, J. Displacement mechanism of oil in shale inorganic nanopores by supercritical carbon dioxide from molecular dynamics simulations. *Energy Fuels* **2017**, *31*, 738–746. [\[CrossRef\]](#)
16. Matkivskiy, S.; Kondrat, O. Studying the influence of the carbon dioxide injection period duration on the gas recovery factor during the gas condensate fields development under water drive. *Min. Miner. Depos.* **2021**, *15*, 95–101. [\[CrossRef\]](#)
17. Matkivskiy, S. Increasing hydrocarbon recovery of Hadiach field by means of CO<sub>2</sub> injection as a part of the decarbonization process of the energy sector in Ukraine. *Min. Miner. Depos.* **2022**, *16*, 114–120. [\[CrossRef\]](#)
18. Zhang, K.; Li, S.; Liu, L. Optimized foam-assisted CO<sub>2</sub> enhanced oil recovery technology in tight oil reservoirs. *Fuel* **2020**, *267*, 117099. [\[CrossRef\]](#)
19. Sun, L.; Bai, B.; Wei, B.; Pu, W.; Wei, P.; Li, D.; Zhang, C. Recent advances of surfactant-stabilized N<sub>2</sub>/CO<sub>2</sub> foams in enhanced oil recovery. *Fuel* **2019**, *241*, 83–93. [\[CrossRef\]](#)

20. Bai, M.; Zhang, Z.; Chen, Q.; Weifeng, S.; Du, S. Research on the Enhanced Oil Recovery Technique of Horizontal Well Volume Fracturing and CO<sub>2</sub> Huff-n-Puff in Tight Oil Reservoirs. *ACS Omega* **2021**, *6*, 28485–28495. [[CrossRef](#)] [[PubMed](#)]
21. Zuo, M.; Chen, H.; Qi, X.; Liu, X.; Xu, C.; Yu, H.; Brahim, M.S.; Wu, Y.; Liu, H. Effects of CO<sub>2</sub> injection volume and formation of in-situ new phase on oil phase behavior during CO<sub>2</sub> injection for enhanced oil recovery (EOR) in tight oil reservoirs. *Chem. Eng. J.* **2022**, *452*, 139454. [[CrossRef](#)]
22. Cheng, H.; Ma, P.; Dong, G.; Zhang, S.; Wei, J.; Qin, Q. Characteristics of Carboniferous Volcanic Reservoirs in Beisantai Oilfield, Junggar Basin. *Math. Probl. Eng.* **2022**, *2022*, 7800630. [[CrossRef](#)]
23. Rajkumar, P.; Pranesh, V.; Kesavakumar, R. Influence of CO<sub>2</sub> retention mechanism storage in Alberta tight oil and gas reservoirs at Western Canadian Sedimentary Basin, Canada: Hysteresis modeling and appraisal. *J. Pet. Explor. Prod. Technol.* **2021**, *11*, 327–345. [[CrossRef](#)]
24. Baban, A.; Keshavarz, A.; Amin, R.; Iglauder, S. Residual Trapping of CO<sub>2</sub> and Enhanced Oil Recovery in Oil-Wet Sandstone Core—A Three-Phase Pore-Scale Analysis Using NMR. *Fuel* **2023**, *332*, 126000. [[CrossRef](#)]
25. Lake, L.W.; Lotfollahi, M.; Bryant, S.L. CO<sub>2</sub> enhanced oil recovery experience and its messages for CO<sub>2</sub> storage. In *Science of Carbon Storage in Deep Saline Formations*; Elsevier: Amsterdam, The Netherlands, 2019; pp. 15–31.
26. Han, J.; Cheng, H.; Shi, Y.; Wang, L.; Song, Y.; Zhnag, W. Connectivity analysis and application of fracture cave carbonate reservoir in Tazhong. *Sci. Technol. Eng.* **2016**, *16*, 147–152.
27. Milad, M.; Junin, R.; Sidek, A.; Imqam, A.; Tarhuni, M. Huff-n-puff technology for enhanced oil recovery in shale/tight oil reservoirs: Progress, gaps, and perspectives. *Energy Fuels* **2021**, *35*, 17279–17333. [[CrossRef](#)]
28. Huang, X.; Li, A.; Li, X.; Liu, Y. Influence of typical core minerals on tight oil recovery during CO<sub>2</sub> flooding using the nuclear magnetic resonance technique. *Energy Fuels* **2019**, *33*, 7147–7154. [[CrossRef](#)]
29. Hou, Z.K.; Cheng, H.L.; Sun, S.W.; Chen, J.; Qi, D.Q.; Liu, Z.B. Crack propagation and hydraulic fracturing in different lithologies. *Appl. Geophys.* **2019**, *16*, 243–251. [[CrossRef](#)]
30. Deveci, M.; Demirel, N.Ç.; John, R.; Özcan, E. Fuzzy multi-criteria decision making for carbon dioxide geological storage in Turkey. *J. Nat. Gas Sci. Eng.* **2015**, *27 Pt 2*, 692–705. [[CrossRef](#)]
31. Bai, J.; Liu, H.; Wang, J.; Qian, G.; Peng, Y.; Gao, Y.; Yan, L.; Chen, F. CO<sub>2</sub>, water and N<sub>2</sub> injection for enhanced oil recovery with spatial arrangement of fractures in tight-oil reservoirs using huff-n-puff. *Energies* **2019**, *12*, 823. [[CrossRef](#)]
32. Alvarado, V.; Manrique, E. Enhanced oil recovery: An update review. *Energies* **2010**, *3*, 1529–1575. [[CrossRef](#)]
33. Cheng, H.; Wei, J.; Cheng, Z. Study on sedimentary facies and reservoir characteristics of Paleogene sandstone in Yingmaili block, Tarim basin. *Geofluids* **2022**, *2022*, 1445395. [[CrossRef](#)]
34. Mahzari, P.; Jones, A.P.; Oelkers, E.H. Impact of in-situ gas liberation for enhanced oil recovery and CO<sub>2</sub> storage in liquid-rich shale reservoirs. *Energy Sources Part A Recovery Util. Environ. Eff.* **2020**, *1–21*. [[CrossRef](#)]
35. Kashkooli, S.B.; Gandomkar, A.; Riazi, M.; Tavallali, M.S. Coupled optimization of carbon dioxide storage and CO<sub>2</sub> enhanced oil recovery. *J. Pet. Sci. Eng.* **2022**, *208*, 109257. [[CrossRef](#)]

**Disclaimer/Publisher’s Note:** The statements, opinions and data contained in all publications are solely those of the individual author(s) and contributor(s) and not of MDPI and/or the editor(s). MDPI and/or the editor(s) disclaim responsibility for any injury to people or property resulting from any ideas, methods, instructions or products referred to in the content.